

A coupled ice-ocean ecosystem model for 1-D and 3-D applications in the Bering and Chukchi Seas

Jin Meibing¹, Clara Deal¹ and Wang Jia²

¹ International Arctic Research Center, University of Alaska Fairbanks, USA

² Great Lakes Environmental Research Lab, NOAA, USA

Received September 20, 2008

Abstract Primary production in the Bering and Chukchi Seas is strongly influenced by the annual cycle of sea ice. Here pelagic and sea ice algal ecosystems coexist and interact with each other. Ecosystem modeling of sea ice associated phytoplankton blooms has been understudied compared to open water ecosystem model applications. This study introduces a general coupled ice-ocean ecosystem model with equations and parameters for 1-D and 3-D applications that is based on 1-D coupled ice-ocean ecosystem model development in the landfast ice in the Chukchi Sea and marginal ice zone of Bering Sea. The biological model includes both pelagic and sea ice algal habitats with 10 compartments: three phytoplankton (pelagic diatom, flagellates and ice algae; D , F , and Ai), three zooplankton (copepods, large zooplankton, and microzooplankton; ZS , ZL , ZP), three nutrients (nitrate + nitrite, ammonium, silicon; NO_3 , NH_4 , Si) and detritus (Det). The coupling of the biological models with physical ocean models is straightforward with just the addition of the advection and diffusion terms to the ecosystem model. The coupling with a multi-category sea ice model requires the same calculation of the sea ice ecosystem model in each ice thickness category and the redistribution between categories caused by both dynamic and thermodynamic forcing as in the physical model. Phytoplankton and ice algal self-shading effect is the sole feedback from the ecosystem model to the physical model.

Key words ecosystem model, sea ice, ocean, ice algae, phytoplankton.

1 Introduction

The Bering and Chukchi Seas are important high-latitude ecosystems that are subject to amplified global warming effects. The contribution of sea ice associated primary production to the annual production increases from the seasonally ice covered Bering, Chukchi and coastal Beaufort Seas to the perennially ice covered central basin of the Arctic Ocean. The rising temperature and reducing sea ice cover in the Bering Sea in recent years has profoundly impacted the ecosystem in many ways, such as shifting the timing and magnitude of the sea ice algal and other pelagic phytoplankton production, and their contribution to the pelagic and benthic food webs^[1-3]. Ecosystem changes have also been reported for the Chukchi Sea. Ice-associated phytoplankton blooms are important, not only because of their contribution to the annual primary production, but also because of their role in timing, mag-

nitude and duration of the open water bloom later in the season. The factors controlling the sea ice ecosystem are still poorly understood compared to those controlling the water column ecosystem. This is due to scarce observations and complexities involving a number of environmental factors, such as ice types and the patchiness of snow and ice thickness distributions. A modeling approach is necessary to understand and examine the differences between observations made at different locations and times (i. e. , different climate regimes). The ecosystem model must include both sea ice algae and pelagic phytoplankton components, if it is to capture both ice-associated and open-water phytoplankton blooms in different regions and times. Thus, the model can be used to assess the effects of global climate changes on ecosystem and its feedbacks by changing carbon production and fixation, DMS production etc.

Previous lower trophic level ecosystem modeling studies in the Bering Sea considered the impacts of physical forcing on the pelagic ecosystem, but did not include sea ice or ice algal components^[4-6]. Few ecosystem models including sea ice algae exist. The growth behavior of the algal community in the fast ice of McMurdo Sound, Antarctica, has been simulated by 1-D ice ecosystem models developed by Arrigo *et al.* (1993)^[7] and Arrigo and Sullivan (1994)^[8]. Primary production of the Antarctic Ocean was estimated by applying this model to distinct locations^[9]. Nishi and Tabeta (2005)^[10] developed a coupled ice-ocean ecosystem model to study the contribution of ice algae to the ice-covered ecosystem of Lake Saroma, and found that ice algae released from the ice are rapidly exported because they sink quickly and the lake is shallow. Carbon flows through the microbial food web of first-year ice in Resolute Passage (Canadian High Arctic) were inferred by Vezina *et al.* (1997)^[11] using an inverse model. A coupled snow-ice-ice algae model was developed by Lavoie *et al.* (2005)^[12] to investigate the importance of different ice algal growth-limitation terms, as well as different loss terms, in regulating the ice algal biomass accumulation at the bottom of landfast ice in the Canadian Archipelago.

Based on biophysical ice core data collected in the landfast ice off Barrow, Alaska in the spring time of 2002 and 2003, Jin *et al.* (2006b)^[13] developed a coupled ice-ocean ecosystem model to study the factors controlling the landfast ice-ocean ecosystem, the processes which release ice algae from the ice bottom, the primary production of ice algae and the export of ice algae to benthos. But due to limited data availability, the model studies were only applied to the sea ice cover period. Jin *et al.* (2007)^[3] applied this 1-D ice-ocean ecosystem in the southeastern Bering Sea to demonstrate how the sea ice algal productions can be linked with and affect the sequential open water phytoplankton blooms.

While the above model applications have had success in simulating the 1-D ice-ocean coupled ecosystem, a systematic description of the coupled model equations and how they can be applied in a 3-D model domain has not been discussed in these previous studies. These topics are the main purpose of this paper. Importantly, the Arctic and Antarctic sea ice packs are mixtures of open water, thin first-year ice, thicker multiyear ice, and thick pressure ridges. The thermodynamic and dynamic properties of the ice pack depend on how much ice lies in each thickness range. Thus the basic problem in sea ice modeling is to describe the evolution of the ice thickness distribution (ITD) in time and space. Exchange and redistribution of biological variables between different ice thickness categories within a model grid cell still need to be studied and justified with observations. Therefore, this pa-

per discusses how to set up a coupled ice-ocean-ecosystem model in a 3-D setting and how to couple this model with physical ocean and sea ice models. The parameters and processes related to the coupled biological models are discussed according to observations and previous modeling studies in the Bering and Chukchi Seas. Applications of the model to other seas or the global oceans are possible if proper attention is paid to the regional differences of some parameters.

2 Coupled ice-ocean ecosystem model

The ecosystem model consists of physical and biological submodels for the water column and sea ice. There exist several types of 3-D coupled ice-ocean models that are based on different types of ocean and sea ice models, such as those in the Arctic Ocean coupled ice-ocean Model Inter-comparison Project (AOMIP, Holloway *et al.* 2007^[14]). Our ecosystem model has been tested to be coupled with the IARC Coupled Ice-Ocean Model (CIOM, Wang 2005^[15]) and the Parallel Ocean Program (POP) and Los Alamos National Laboratory (LANL) sea ice model (CICE, Hunke and Lipscomb 2006^[16]).

The physical model equations and their numerical solutions have been extensively documented in the literature and therefore are omitted in this paper, except for illustrating the coupling with biological models. The focus of this study is the coupled ice-ocean biological model and its coupling with the physical model in both vertically 1-D and 3-D forms.

The biological model equations are described in two parts as in the flowchart of the biological compartments (Figure 1): sea ice and sea water. The following sections introduce the model equations in vertically 1-D form first and then their coupling with the 1-D and 3-D physical models.

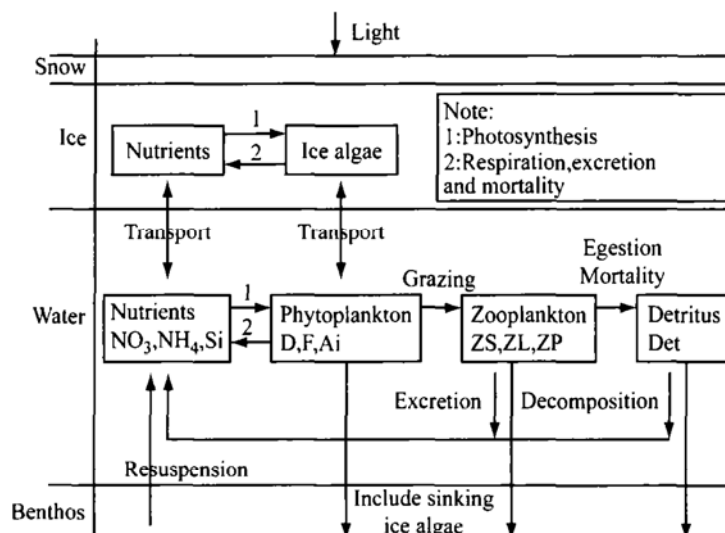


Fig. 1 Flowchart of the coupled ice-ocean ecosystem model (biological component only).

2.1 The sea ice ecosystem model equations and coupling with physical sea ice model

Ice core data showed that most of ice algal biomass is concentrated at the bottom skeletal layer, because of the stable environment that is favorable for growth. The upward distri-

bution of ice algae is limited by nutrient availability and the high brine salinity characteristic of the sea ice interior when temperatures are low^[17]. Therefore, the ice algae are calculated only at the bottom layer of the sea ice. In the previous studies^[3–13], this layer is 2 cm thick, but it is adjustable in the model if more observations prove that the active layer of ice algal growth is different.

Zooplankton grazing in the sea ice is still under studied, and is not included in Jin *et al.* (2006b)^[13], because the grazing pressure of sea-ice meiofauna is low compared to daily primary production rates of less than 5% / day^[18,19]. Similarly, grazing impact on the ice-algal standing stock at the ice underside in summer is low, e. g., 1.1% in the Laptev Sea and 2.6% in the Greenland Seas^[20]. But the grazing of ice algae in the water is included similar to diatom in the Bering Sea^[3]. Although the ice bottom grazing has been observed, a quantitative description of the process is undeveloped. Thus, zooplankton grazing is not included in sea ice ecosystem model equations.

2.1.1 The biological equations

The biological model in the sea ice includes four compartments (ice algae; A_i ; in units of mmol N/m³, and three nutrients: NO_3 , NH_4 , and Si in units of mmol N/m³, mmol N/m³ and mmol Si/m³, respectively) in one layer at the bottom of sea ice. The biological equations follows Jin *et al.* (2006b)^[13]:

$$\frac{\partial A_i}{\partial t} = A_i(G^{A_i} - R^{A_i} - R_e^{A_i}) + \frac{\partial T_{wi} A_i}{\partial z} + \frac{\partial}{\partial z} \left(K_{wi} \frac{\partial A_i}{\partial z} \right) \quad (1)$$

$$\frac{\partial NO_3}{\partial t} = C_{AtoN} \cdot NH_4 - f_{NO_3} A_i(G^{A_i} - R^{A_i}) + \frac{\partial T_{wi} NO_3}{\partial z} + \frac{\partial}{\partial z} \left(K_{wi} \frac{\partial NO_3}{\partial z} \right) \quad (2)$$

$$\frac{\partial NH_4}{\partial t} = A_i R_g^{A_i} - (1 - f_{NO_3}) A_i(G^{A_i} - R^{A_i}) - C_{AtoN} \cdot NH_4 + \frac{\partial T_{wi} NH_4}{\partial z} + \frac{\partial}{\partial z} \left(K_{wi} \frac{\partial NH_4}{\partial z} \right) \quad (3)$$

$$\frac{\partial Si}{\partial t} = -k_{Si} A_i(G^{A_i} - R^{A_i}) + \frac{\partial T_{wi} Si}{\partial z} + \frac{\partial}{\partial z} \left(K_{wi} \frac{\partial Si}{\partial z} \right) \quad (4)$$

where N_{frac} , Si_{frac} , I_{frac} are ratios expressing nitrogen, silicon and light limitation. K_{wi} is the molecular diffusion coefficient between the liquid in the bottom layer of sea ice and sea surface layer. Terms G^{A_i} , R^{A_i} , $R_g^{A_i}$ are phytoplankton growth rate, respiration rate, and mortality rate, respectively.

$$G^{A_i} = \mu_0^{A_i} e^{0.0633T_i} \times \min(N_{frac}, Si_{frac}, I_{frac}) \xi; R^{A_i} = 0.05 \mu_0^{A_i} e^{rT_i}; R_g^{A_i} = R_{g0} e^{r_g T_i} \quad (5,6,7)$$

$$N_{frac} = \frac{NO_3}{K_{SNO_3}^{A_i} + NO_3} e^{-\psi NH_4} + \frac{NH_4}{K_{SNH_4}^{A_i} + NH_4}; Si_{frac} = \frac{Si}{K_{SSi}^{A_i} + Si} \quad (8,9)$$

$$I_{frac} = (1 - e^{-I\alpha^{A_i}/P_{max}}) e^{-I\beta^{A_i}/P_{max}} \quad (10)$$

$$f_{NO_3} = \left(\frac{NO_3}{K_{SNO_3} + NO_3} e^{-\psi NH_4} \right) / N_{frac} \quad (11)$$

where T_i is the temperature in the bottom 2 cm skeletal layer. Term ξ is an empirical salinity-dependent ice algal growth rate calculated as in Arrigo and Sullivan (1992)^[17]. Brine flux volume in the skeletal layer has a high correlation ($R^2 = 0.994$) with ice growth rate (dH_{ice}/dt) during the ice growth period^[21]. The water-ice interface transport T_{wi} is calcu-

lated using (11a) during ice growth period and (11b) during ice melt^[13]:

$$T_{wi} = C_{wi} \left[9.667 \times 10^{-9} + 4.49 \times 10^{-4} \frac{dH_{ice}}{dt} - 1.39 \times 10^{-3} \left(\frac{dH_{ice}}{dt} \right)^2 \right] \quad (12a)$$

$$T_{wi} = C_{wi} \left[4.49 \times 10^{-4} \frac{dH_{ice}}{dt} - 1.39 \times 10^{-3} \left(\frac{dH_{ice}}{dt} \right)^2 \right] \quad (12b)$$

where the coefficients have been adjusted for metric units and T_{wi} is expressed in units of ms^{-1} . C_{wi} is a constant coefficient which is a combination of many factors, such as the fraction of the skeletal layer that is open to convection, layer depth etc. Its value was determined according to model-data comparison: C_{wi} is 72 during ice growth and 720 during ice melt^[13]. Table 1 provides a list of parameters used in the sea ice ecosystem model, their units, and values.

Table 1. List of parameter values for sea ice ecosystem model^[3-13]

Symbol (definition)/Unit	Value
R_{G0} (maximum phytoplankton mortality rate at 0 °C)/h ⁻¹	9.23×10^{-4}
r, r_g (temperature coefficients)/Deg ⁻¹	0.0633, 0.03
μ_0^{Ai} (maximum growth rate at 0 °C)/h ⁻¹	0.06
C_{AtoN} (nitrification factor)/d ⁻¹	0.015
k_{Si} (silicon to nitrogen mole ratio)/Si:N	1.8
$K_{SNO_3}^{Ai}, K_{SNH_4}^{Ai}$ /μM · N	1, 1
K_{SSi}^{Ai} /μM · Si	4
Ψ /(mmol · N) ⁻¹ m ³	1.46
α^{Ai}/P_{max} (light-limited slope/maximal photosynthetic rate)/W ⁻¹ m ²	0.8
β^{Ai}/P_{max} (slope of light inhibition/maximal rate)/W ⁻¹ · m ²	0.018
W^{Ai} (sinking velocity of ice algae within sea ice)/m/h	0
K_{wi} (diffusion coefficient at water and ice interface)/m/s ²	10^{-5}

2.1.2 Coupling with sea ice model

In vertically 1-D case, only one column of sea ice is calculated and the coupling only requires the following variables from the physical model or observations: ice thickness and vertically distribution of temperature, salinity, and light intensity. Thus, the coupling is a direct utilization of those physical outputs and does not involve any new equations to be solved.

In 3-D case, the coupling is complicated by the mixtures of open water, thin first-year ice, thicker multiyear ice, and thick pressure ridges in the Arctic and Antarctic sea ice packs. Most of the existing sea ice models use multi-category ice thickness method to compute the thermodynamic and dynamic properties of the different ice packs in each grid cell (such as CICE by Hunke and Lipscomb, 2006^[16]; CIOM by Wang *et al.* 2005^[15]; etc.). Therefore, biological variables must be calculated in each category within a grid cell. The exchange and redistribution of any scalar variables between categories are tied with the ice thickness distribution function g governed by:

$$\frac{\partial g}{\partial t} = -\frac{\partial g u_i}{\partial x} - \frac{\partial g v_i}{\partial y} - \frac{\partial f_i g}{\partial h} + \Psi \quad (13)$$

where u_i, v_i are the horizontal ice velocity, f_i is the rate of thermodynamic ice growth, and Ψ is a ridging redistribution function due to ice convergence. If number of categories is NC and the ice thickness in each category is centered with $h = h_1, h_2, \dots, h_{NC}$, then $g(h_n)$ is defined as the fractional area covered by ice in the thickness range centered with h_n at a given time and location. Usually, the first category is defined as open water with $h_1 = 0$. The average ice thickness \bar{h} and ice concentration A in a grid cell is therefore expressed as

$$\bar{h} = \sum_{n=2}^{NC} g(h_n) h_n; A = 1 - g(h = 0) \quad (14,15)$$

From the above equations, the ice thickness distribution function and thus ice thickness can be changed due to both thermodynamic (growth and melt) and dynamic (advection and ridging) reasons, but only the thermodynamic caused ice growth rate can cause the water-ice interface transport T_{wi} in the ecosystem model. Therefore, the ice growth rate (dH_{ice}/dt) in the ecosystem model refers to thermodynamic related and should be equal to f_i in the sea ice model, which is calculated by balancing the heat budget on the upper ice surface and the oceanic heat flux out of the ocean surface in the coupled ice-ocean model. While $d\bar{h}/dt$ denotes a composite growth rate of the mean ice thickness in a grid cell caused by both thermodynamic and dynamic reasons.

The 1-D biological model is calculated in each ice category with the physical input of ice thickness growth rate and vertical distribution of temperature, salinity, and light intensity. For any biological variable b in the bottom of sea ice, its mean in a grid cell is expressed similar to (14):

$$\bar{b} = \sum_{n=2}^{NC} g(h_n) b_n \quad (16)$$

The horizontal advection is calculated for each ice category using the same numerical scheme of the sea ice dynamic model:

$$\frac{\partial b}{\partial t} = -\frac{\partial b u_i}{\partial x} - \frac{\partial b v_i}{\partial y} \quad (17)$$

The redistribution of ice in thickness space occurs during both thermodynamic ice growth/melt and dynamic ice ridging (including other mechanical processes) that convert thinner ice to thicker ice. Those processes cause the biological variables to redistribute between ice categories in the same time. The calculation of those processes must follow the numerical algorithm in the sea ice model and be proportional to the redistribution of g to conserve the mass of biological variables.

2.2 The pelagic ecosystem model equations and coupling with physical ocean model

2.2.1 The biological equations

The pelagic ecosystem model is based on Jin *et al.* (2006a)^[6] with an addition of the ice algal compartment. There are ten compartments in the water column (nine in Jin *et al.* 2006a^[6]): three phytoplankton (diatom, flagellates and ice algae: D , F and Ai), three zooplankton (small copepods, large copepods, and microzooplankton: ZS , ZL , ZP), three nutrients (nitrate + nitrite, ammonium, silicon: NOB_3 , NHB_4 , Si) and detritus (Det). The biological model equations consist of biological source/sink terms plus a physical ad-

vection and diffusion term at the end of each equation that will be used in the coupling with physical ocean model:

$$\frac{\partial Ai}{\partial t} = Ai(G^{Ai} - R^{Ai} - Rg^{Ai}) - \Gamma^{AiS} ZS - \Gamma^{AiL} ZL - \Gamma^{AiP} ZP + \frac{\partial(W^{Ai} Ai)}{\partial z} + \Phi_{Ai} \quad (18)$$

$$\frac{\partial D}{\partial t} = D(G^D - R^D - Rg^D) - \Gamma^{DS} ZS - \Gamma^{DL} ZL - \Gamma^{DP} ZP + \frac{\partial(W^D D)}{\partial z} + \Phi_D \quad (19)$$

$$\frac{\partial F}{\partial t} = F(G^F - R^F - Rg^F) - \Gamma^{FS} ZS - \Gamma^{FL} ZL - \Gamma^{FP} ZP + \frac{\partial(W^F F)}{\partial z} + \Phi_F \quad (20)$$

$$\frac{\partial ZS}{\partial t} = ZS[A^S(\Gamma^{DS} + \Gamma^{FS} + \Gamma^{AiS} + \Gamma^{PS})(1 - Ex^S) - M^S] + \Phi_{ZS} \quad (21)$$

$$\frac{\partial ZL}{\partial t} = ZL[A^L(\Gamma^{DL} + \Gamma^{FL} + \Gamma^{AiL} + \Gamma^{PL})(1 - Ex^L) - M^L] + \frac{\partial(W^L ZL)}{\partial z} + \Phi_{ZL} \quad (22)$$

$$\frac{\partial ZP}{\partial t} = ZP[A^P(\Gamma^{DP} + \Gamma^{AiP} + \Gamma^{FP})(1 - Ex^P) - M^P] - \Gamma^{PS} ZS - \Gamma^{PL} ZL + \Phi_{ZP} \quad (23)$$

$$\frac{\partial NO_3}{\partial t} = -f_{NO_3}[D(G^D - R^D) + F(G^F - R^F) + Ai(G^{Ai} - R^{Ai})] + C_{AtoN} \cdot NH_4 + \Phi_{NO_3} \quad (24)$$

$$\begin{aligned} \frac{\partial NH_4}{\partial t} = & ZS \cdot A^S(\Gamma^{DS} + \Gamma^{FS} + \Gamma^{AiS} + \Gamma^{PS})Ex^S + ZL \cdot A^L(\Gamma^{DL} + \Gamma^{FL} + \Gamma^{AiL} + \Gamma^{PL})Ex^L \\ & + \\ & ZP \cdot A^P(\Gamma^{DP} + \Gamma^{FP} + \Gamma^{AiP})Ex^M + D \cdot Rg^D + F \cdot Rg^F + Ai \cdot Rg^{Ai} + Det \cdot Rg^{Det} - \\ & (1 - f_{NO_3})[D(G^D - R^D) + F(G^F - R^F) + Ai(G^{Ai} - R^{Ai})] - C_{AtoN} \cdot NH_4 + \Phi_{NH_4} \end{aligned} \quad (25)$$

$$\frac{\partial Si}{\partial t} = -\kappa_{Si}[D(G^D - R^D) + Ai(G^{Ai} - R^{Ai})] + \Phi_{Si} \quad (26)$$

$$\begin{aligned} \frac{\partial Det}{\partial t} = & ZS \cdot [(1 - A^S)(\Gamma^{DS} + \Gamma^{FS} + \Gamma^{AiS} + \Gamma^{PS}) + M^S] + \\ & ZL \cdot [(1 - A^L)(\Gamma^{DL} + \Gamma^{FL} + \Gamma^{AiL} + \Gamma^{PL}) + M^L] + \\ & ZP \cdot [(1 - A^P)(\Gamma^{DP} + \Gamma^{FP} + \Gamma^{AiP}) + M^P] - Det \cdot Rg^{Det} + \frac{\partial(W^{Det} Det)}{\partial z} + \Phi_{Det} \end{aligned} \quad (27)$$

where superscripts *D*, *F* and *Ai* denote diatoms, flagellates and ice algae in the water column. Superscripts *S*, *L*, and *P* denote small copepods, large copepods, and micro-zooplankton. Terms *G*, *R*, *Rg* are phytoplankton growth rate, respiration rate, and mortality rate, respectively.

$$G^X = \mu_0^X e^{rT} \times \min(N_{frac}, Si_{frac}, I_{frac}) \quad (\text{for diatom and flagellate}) \quad (28a)$$

$$G^{Ai} = \mu_0^{Ai} e^{T_{freeze} - T} \times \min(N_{frac}, Si_{frac}, I_{frac}) \xi \quad (\text{for ice algae by Jin et al. (2007)}) \quad (28b)$$

$$R^X = 0.05\mu_0^X e^{rT}; Rg^X = Rg_0 e^{r_s T} \quad (28c, d)$$

The superscript *X* denotes *D*, *F* or *Ai*. μ_0^X is maximum phytoplankton growth rate at 0°C. T_{freeze} is the freezing temperature of the sea water. $N_{frac}, Si_{frac}, I_{frac}$ are unitless ratios expressing nitrogen, silicon and light limitation as defined in Eslinger *et al* (2001)^[4]. Si_{frac}

is only used for diatoms. Γ^{XY} denote the grazing rate of zooplankton Y on phytoplankton X , formulated as modified Ivlev-type grazing with temperature dependant rates, similar rates are also applied to small and large zooplankton Y (ZS and ZL) grazing on microzooplankton $X(ZP)^{[4-22]}$:

$$\Gamma^{XY} = \Gamma_{XY}(1 - e^{-\lambda_{XY}(X-X_Y)})e^{rT} \quad (29)$$

Zooplankton grazing rate is also expressed as temperature dependant:

$$M^Y = M_0^Y e^{rT} \quad (30)$$

The sinking rate of phytoplankton and zooplankton (W^X , W^Y), the remineralization rate of detritus (Rg^{Det}), and the ratio of phytoplankton growth due to nitrate uptake to that due to both nitrate and ammonium uptake (f_{NO_3}) follow Eslinger *et al.* (2001)^[4]. Silicon losses due to uptake are restored back to the bottom layer instantly^[6], that conserves the silicon in the whole water column. This is important for the model to run longer than one season.

The equations for calculating N_{frac} , Si_{frac} , I_{frac} of diatom and flagellate are in the same form as (8) to (10) for ice algae, just with different parameter values (Table 2). Table 2 provides a list of parameters used in the pelagic ecosystem model, their units, and values.

Table 1. List of parameter values for pelagic ecosystem model in sea water^[3-6].

Symbol (definition)/Unit	Value
Rg_0 (maximum phytoplankton mortality rate at 0°C)/h ⁻¹	9.23×10^{-4}
R , r_g (temperature coefficients)/Deg ⁻¹	0.0633, 0.03
$\Gamma_{DS}, \Gamma_{DL}, \Gamma_{DP}, \Gamma_{FS}, \Gamma_{FL}, \Gamma_{FP}, \Gamma_{AIS}, \Gamma_{AIL}, \Gamma_{AIP}, \Gamma_{PS}, \Gamma_{PL}$ (Ivlev-type grazing constants)/h ⁻¹	0.005, 0.003, 0.01, 0.013, 0.003, 0.01, 0.005, 0.003, 0.01, 0.01, 0.01
$\lambda_{DS}, \lambda_{DL}, \lambda_{DP}, \lambda_{FS}, \lambda_{FL}, \lambda_{FP}, \lambda_{AIS}, \lambda_{AIL}, \lambda_{AIP}, \lambda_{PS}, \lambda_{PL}$ (Ivlev-type grazing constants)/ μM^{-1}	1.50, 2.73, 2.73, 2.73, 2.73, 2.73, 1.50, 2.73, 2.73, 2.73, 2.73
$D_S, D_L, D_P, F_S, F_L, F_P, A_{IS}, A_{IL}, A_{IP}, P_S, P_L$ (Ivlev-type grazing constants)/ $\mu M \cdot N$	0.25, 0.50, 0.50, 0.25, 0.50, 0.50, 0.25, 0.50, 0.50, 0.25, 0.25
A^Y (assimilation ratio of grazed phytoplankton)	0.7
Ex^Y (egestion ratio of grazed phytoplankton)	0.4
M_0^Y (natural mortality rate of zooplankton at 0 °C)/d ⁻¹	0.06
κ_{Si} (silicon to nitrogen mass ratio for diatoms)	1.104
$\mu_0^D, \mu_0^F, \mu_0^{Ai}$ (Maximum phytoplankton growth rate at 0 °C)/h ⁻¹	0.07, 0.038, 0.07
$K_{SNO_3}^D, K_{SNH_4}^D, K_{SNO_3}^F, K_{SNH_4}^F$ /μM · N	2.5, 2.5, 0.6, 0.6
K_{SSi}^D, K_{SSi}^F /μM · Si	3, 3
$\alpha^D/P_{max}, \alpha^F/P_{max}$ (light-limited slope/maximal photosynthetic rate)/W ⁻¹ · m ²	0.0536, 0.0536
$\beta^D/P_{max}, \beta^F/P_{max}$ (slope of light inhibition/maximal rate)/W ⁻¹ · m ²	1.795e-3, 1.795e-3

2.2.2 Coupling with ocean model

The pelagic ecosystem model equations (18)-(27) already include the advection and diffusion terms Φ at the end of each equation, which is defined as the following operator on the corresponding biological compartment:

$$\Phi = \frac{\partial}{\partial x} \left(A_H \frac{\partial}{\partial x} \right) + \frac{\partial}{\partial y} \left(A_H \frac{\partial}{\partial y} \right) + \frac{\partial}{\partial z} \left(K_H \frac{\partial}{\partial z} \right) - u \frac{\partial}{\partial x} - v \frac{\partial}{\partial y} - w \frac{\partial}{\partial z} \quad (31)$$

In vertically 1-D applications, only the derivatives along z-direction in the above equa-

tion are used. The transport across the water-ice interface is supplied as the upper (lower) boundary conditions for the pelagic (sea ice) ecosystem models. The algorithm is that the bottom layer of the sea ice ecosystem model is considered to a layer above the sea surface, but with molecular diffusion coefficient and vertical velocity specified by T_{wi} in the sea ice ecosystem model.

The ecosystem model can have one feedback to the ocean model by applying the phytoplankton and ice algae self-shading effects in the calculation of the light attenuation coefficient in the physical model. E. g. , the self-shading coefficients of ice algae in the sea ice and phytoplankton are 0.005 and $0.015 \text{ m}^2 (\text{mmol} \cdot \text{N})^{-1}$ in our previous studies^[6-13].

3 Model applications and discussion

The pelagic ecosystem model has been applied in both 1-D and 3-D using an earlier version of the ecosystem model^[6,13,23]. The coupled ice-ocean ecosystem model has been successful in 1-D applications on the landfast ice offshore Barrow in Chukchi Sea and the NOAA/PMEL mooring site 2 of the southeastern Bering Sea^[3-13]. In Jin *et al.* (2007)^[3], only the years (1997 and 1999) with ice-associated phytoplankton blooms were discussed. Here we show the comparison of fluorometer data with simulated total phytoplankton from 1997 to 2002 (Figure 2) to demonstrate the model performance on the following aspects: 1) a continuous model run can reproduce the annual events of phytoplankton blooms in the region; 2) the phytoplankton bloom consists of both ice algae and open water phytoplankton species (diatom and flagellate) and the dominant species change with physical environments (i. e. , temperature, timing of sea ice presence, wind speed etc.) ; 3) both ice-associated and open water phytoplankton blooms compared well with mooring observations in cold (1997, 1999) and warm years (1998 and 2000 to 2002).

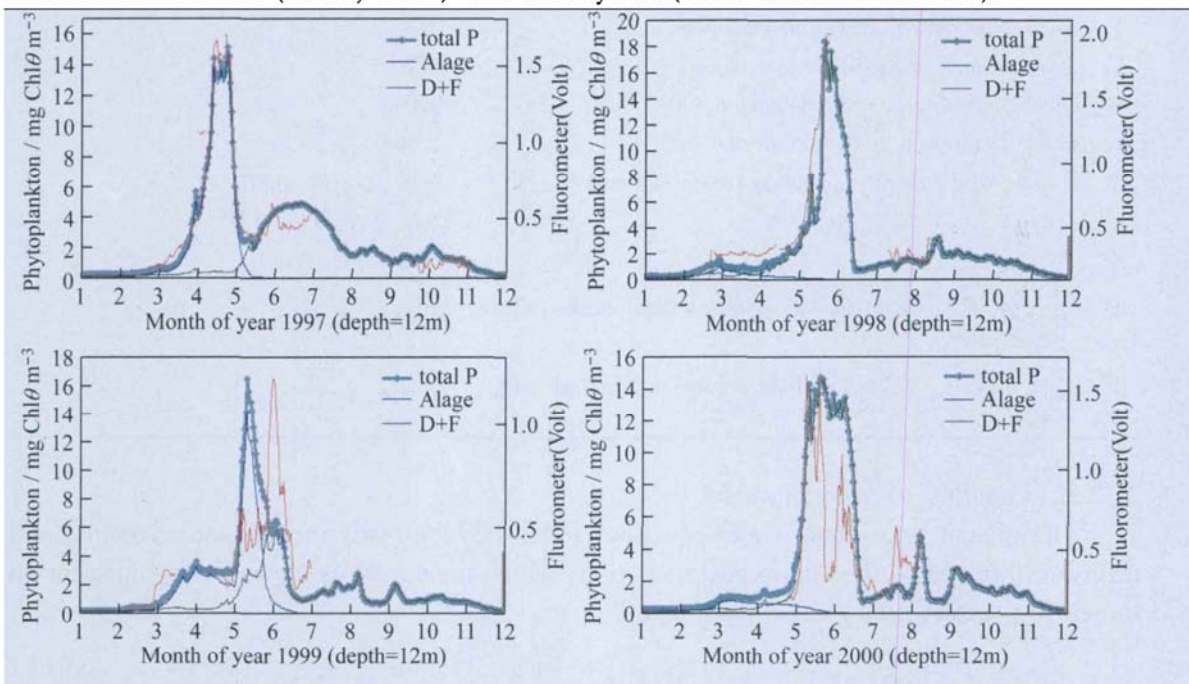


Fig. 2 Comparison of fluorometer with simulated total phytoplankton at 12 m. The ice algal concentration, diatom and flagellate concentration (D + F) are also included.

Implementation of 3-D ice-ocean ecosystem model coupled with POP and CICE is one of our ongoing projects in collaboration with S. Elliott, M. Maltrud and E. Hunke of Los Alamos National Laboratory. Preliminary results of ice algal biomass from the global ecosystem model (Figure 3) when including features of the ice ecosystem model showed the feasibility of the model coupling schemes^[13]. The ice algal biomass in April was consistent with higher in the ice of 60s to 70 degree north, but much lower at higher latitude due to light limitations (Figure 3). The timing of an ice algal bloom outside Barrow in April was constant with observations in Jin *et al.* (2006b)^[13]. The model grid is 1-degree with the north pole displaced to Greenland and the spatial and temporal difference of the biological equations are treated as passive tracer (like temperature and salinity) in the POP and CICE (see user's documents for POP at <http://climate.lanl.gov/Models/POP>, and CICE by Hunke and Lipscomb, 2006^[16]). Although the model is applied to global oceans to avoid the difficulties of providing open boundary conditions in regional applications, our emphasis is on the Bering and Chukchi Seas, and model validation in a wide range of the subarctic and arctic oceans is still under way. Since the parameters introduced in this paper have only been validated against observations in limited regions and cases, it is important to conduct more model validations in different ocean and sea ice conditions. The set of model equations should be suitable for applications in other seas or the global ocean. Once the model scheme and parameters are justified, the coupled ice-ocean ecosystem model will be an important tool to quantify primary production from open water and sea ice habitats, and to evaluate their relative function in regional to global biogeochemical cycling. The model is also important for investigating the response of the polar and subpolar ecosystem to short-term weather variations and long-term global climate change ms.

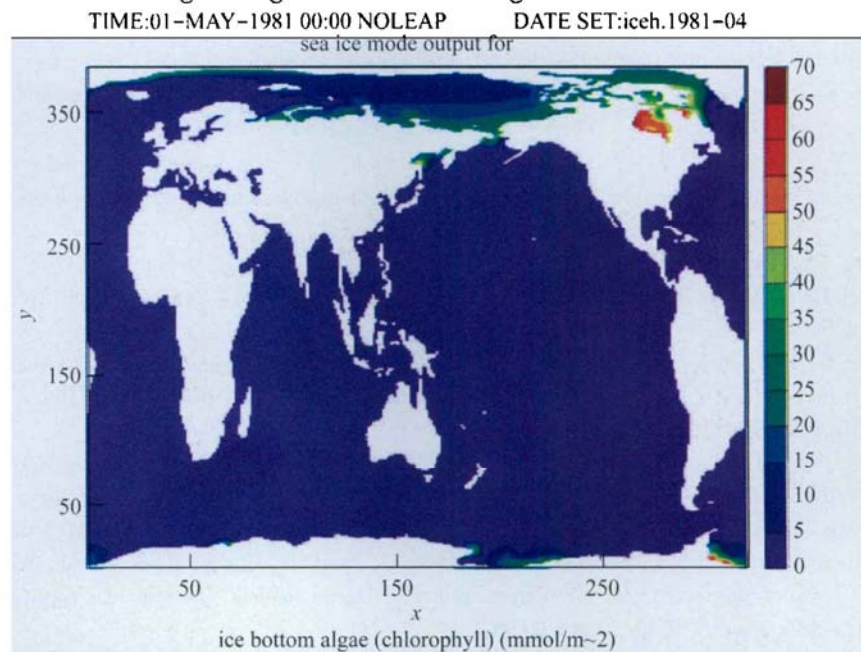


Fig. 3 Ice algal biomass in the bottom 3 cm of sea ice from the 3-D global ecosystem model. Note the concentration should be divided by 0.03 m to be in unit per volume.

Acknowledgements This study was supported by North Pacific Research Board (NPRB) grant 607 (paper contribution number 202), NSF grant ARC – 0652838 and DOE/EPSCoR grant DE – FG02 – 08ER46502. This is GLERL Contribution No. 1499 and DOE/EPSCoR. International Arctic Research Center, University of Alaska Fairbanks supported this study through the JAMSTEC-IARC Research Agreement.

References

- [1] Hunt GL, Stabeno PJ, Walters G, Sinclair E, Brodeur RD, Napp JM, Bond NA (2002): Climate change and control of the southeastern Bering Sea pelagic ecosystem. *Deep-Sea Research II*, 49:5821 – 5853.
- [2] Stabeno PJ, Bond A, Kachel B, Salo A, Schumacher JD (2001): On the temporal variability of the physical environment over the southeastern Bering Sea. *Fisheries Oceanography*, 10(1):81 – 98.
- [3] Jin M, Deal C, Wang J, Alexander V, Gradinger R, Saitoh S, Iida T, Wan Z, Stabeno P (2007): Ice-associated phytoplankton blooms in the southeastern Bering Sea. *Geophysical Research Letter*, 34: L06612 doi:10.1029/2006GL028849.
- [4] Eslinger DL, Iverson RL (2001): The effects of convective and wind-driven mixing on spring phytoplankton dynamics in the Southeastern Bering Sea middle shelf domain. *Continental Shelf Research*, 21: 627 – 650.
- [5] Merico A, Tyrrel T, Lessard EJ, Oguz T, Stabeno PJ, Zeeman SI, Whitledge TE (2004): Modeling phytoplankton succession on the Bering Sea shelf: Role of climate influences and trophic interactions in generating *Emiliana huxleyi* blooms 1997-2000. *Deep-Sea Research*, part I, 51:1803 – 1826.
- [6] Jin M, Deal CJ, Wang J, Tanaka N, Ikeda M (2006a): Vertical mixing effects on the phytoplankton bloom in the southeastern Bering Sea mid-shelf. *J. Geophys. Res.*, 111: C03002, doi:10.1029/2005JC002994.
- [7] Arrigo KR, Kremer JN, Sullivan CW (1993): A simulated Antarctic fast-ice ecosystem. *Journal of Geophysical Research*, 98: 6929 – 6946.
- [8] Arrigo KR, Sullivan CW (1994): A high resolution bio-optical model of microalgal growth: Tests using sea ice algal community time series data. *Limnology and Oceanography*, 39: 609 – 631.
- [9] Arrigo KR, Worthen DL, Lizotte MP, Dixon P, Dieckmann G (1997): Primary production in Antarctic sea ice. *Science*, 276:394 – 397.
- [10] Nishi Y, Tabeta S (2005): Analysis of the contribution of ice algae to the ice-covered ecosystem in Lake Saroma by means of a coupled ice – ocean ecosystem model. *Journal of Marine Systems*, 55: 249 – 270.
- [11] Vezina AF, Demers S, Laurion I, Sime-Ngando T, Juniper SK, Devine L (1997): Carbon flows through the microbial food web of first-year ice in Resolute Passage (Canadian High Arctic). *Journal of Marine Systems*, 11:173 – 189.
- [12] Lavoie D, Denman K, Michel C (2005): Modeling ice algal growth and decline in a seasonally ice-covered region of the Arctic (Resolute Passage, Canadian Archipelago). *J. Geophys. Res.*, 110: C11009, doi: 10.1029.2005JC002922.
- [13] Jin M, Deal CJ, Wang J, Shin KH, Tanaka N, Whitledge TE, Lee SH, Gradinger RR (2006b): Controls of the landfast ice-ocean ecosystem offshore Barrow, Alaska. *Annals of Glaciology*, 44:63 – 72.
- [14] Holloway G, Dupont F, Golubeva E, Hakkinen S, Hunke E, Jin M, Karcher M, Kauker F, Maltrud M, Morales Maqueda MA, Maslowski W, Platov G, Stark D, Suzhki T, Steele M, Wang J, Zhang J (2007): Water properties and circulation in Arctic Ocean models. *Journal of Geophysical Research*, 112:C04S03, doi:10.1029/2006JC003642.
- [15] Wang J, Liu Q, Jin M, Ikeda M, Saucier FJ (2005): A Coupled Ice-Ocean Model in the Pan Arctic and North Atlantic Ocean: Simulations of Seasonal Cycles. *Journal of Oceanography*, 61:213 – 233.
- [16] Hunke EC, Lipscomb WH (2006): CICE: the Los Alamos Sea Ice Model Documentation and Software User's manual. T-3 Fluid Dynamics Group. Los Alamos National laboratory, 1 – 59.

- [17] Arrigo KR, Sullivan CW(1992) :The influence of salinity and temperature covariation on the photophysiological characteristics of Antarctic sea ice microalgae. *J. Phycol.* , 28 : 746 – 756.
- [18] Gradinger R(1999) :Vertical fine structure of algal biomass and composition in Arctic pack ice. *Mar. Biol.* , 133 :745 – 754.
- [19] Michel C, Nielsen TG, Nozais C, Gosselin M(2002) : Significance of sedimentation and grazing by ice micro- and meiofauna for carbon cycling in annual sea ice (northern Baffin Bay). *Aquat Microb Ecol* , 30 :57 – 68.
- [20] Werner I(1997) :Grazing of Arctic under-ice amphipods on sea-ice algae. *Marine Ecology Progress Series* , 160 :93 – 99.
- [21] Wakatsuchi M, Ono N(1983) :Measurements of salinity and volume of brine excluded from growing sea ice. *J. Geophys. Res.* , 88 : 2943 – 2951.
- [22] Ivlev VS(1945) :The biological productive of waters. *Usp. Sovern. Biol.* , 19 :98 – 102.
- [23] Jin M, Wang J, McRoy P(2003) : A 3-D coupled physical-biological model and its application to the spring plankton bloom of 1996 in Prince William Sound, Alaska. *Ecosystems and Sustainable Develop* , WIT press, 81 – 91.